

# Simple multi-dataset detection

Xingyi Zhou<sup>1</sup> Vladlen Koltun<sup>2</sup> Philipp Krähenbühl<sup>1</sup>

## Abstract

How do we build a general and broad object detection system? We use all labels of all concepts ever annotated. These labels span diverse datasets with potentially inconsistent taxonomies. In this paper, we present a simple method for training a unified detector on multiple large-scale datasets. We use dataset-specific training protocols and losses, but share a common detection architecture with dataset-specific outputs. We show how to automatically integrate these dataset-specific outputs into a common semantic taxonomy. In contrast to prior work, our approach does not require manual taxonomy reconciliation. Our multi-dataset detector performs as well as dataset-specific models on each training domain, but generalizes much better to new unseen domains. Entries based on the presented methodology ranked first in the object detection and instance segmentation tracks of the ECCV 2020 Robust Vision Challenge.

## 1. Introduction

Computer vision aims to produce broad, general-purpose perception systems that work in the wild. Yet object detection is fragmented into datasets (Lin et al., 2014; Neuhold et al., 2017; Shao et al., 2019; Kuznetsova et al., 2020) and our models are locked into the corresponding domains. This fragmentation brought rapid progress in object detection (Ren et al., 2015) and instance segmentation (He et al., 2017), but comes with a drawback. Single datasets are limited in both image domains and label vocabularies and do not yield general-purpose recognition systems. Can we alleviate these limitations by unifying diverse detection datasets?

In this paper, we first make training an object detector on a collection of disparate datasets as straightforward as training on a single one. Different datasets are usually trained under different training losses, data sampling strategies, and schedules. We show that we can train a single detector with separate outputs for each dataset, and apply dataset-specific

<sup>1</sup>UT Austin <sup>2</sup>Intel Labs. Correspondence to: Xingyi Zhou <zhouxu@cs.utexas.edu>.

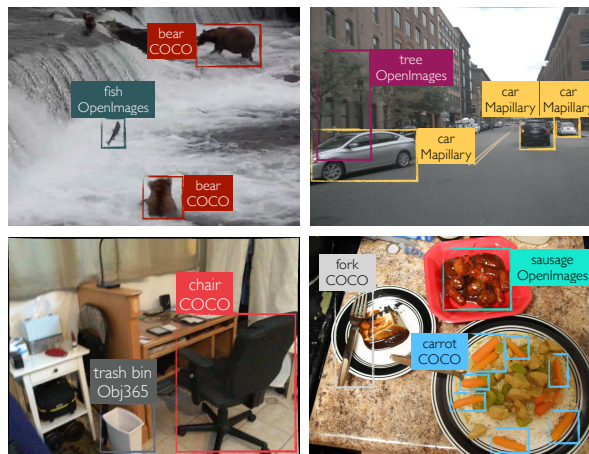


Figure 1. Different datasets span diverse semantic and visual domains. We learn to unify the label spaces of multiple datasets and train a single object detector that generalizes across datasets.

supervision to each. Our training mimics training parallel dataset-specific models with a common network. As a result, our single detector takes full advantages of all training data, performs well on training domains, and generalizes better to new unseen domains. However, this detector produces duplicate outputs for classes that occur in multiple datasets.

A core challenge is integrating different datasets into a common taxonomy, and training a detector that reasons about general objects instead of dataset-specific classes. Traditional approaches create this taxonomy by hand (Lambert et al., 2020; Zhao et al., 2020), which is both time-consuming and error-prone. We present a fully automatic way to unify the output space of a multi-dataset detection system using visual data only. We use the fact that object detectors for similar concepts from different datasets fire on similar novel objects. This allows us to define the cost of merging concepts across datasets, and optimize for a common taxonomy fully automatically. Our optimization jointly finds a unified taxonomy, a mapping from this taxonomy to each dataset, and a detector over the unified taxonomy using a novel 0-1 integer programming formulation. An object detector trained on this unified taxonomy has a large, automatically constructed vocabulary of concepts from all training datasets.

We evaluate our unified object detector at an unprecedented scale. We train a unified detector on 3 large and diverse

datasets: COCO (Lin et al., 2014), Objects365 (Shao et al., 2019), and OpenImages (Kuznetsova et al., 2020). For the first time, we show that a single detector performs as well as dataset-specific models on each individual dataset. A unified taxonomy further improves this detector. Crucially, we show that models trained on diverse training sets generalize zero-shot to new domains, and outperform single-dataset models. Our models ranked first in the object detection and instance segmentation tracks of the ECCV 2020 Robust Vision Challenge across all evaluation datasets. Code and models are release at <https://github.com/xingyizhou/UniDet>.

## 2. Related Work

**Training on multiple datasets.** In recent years, training on multiple diverse datasets has emerged as an effective tool to improve model robustness for depth estimation (Ranftl et al., 2020) and stereo matching (Yang et al., 2019). In these domains, unifying the output space involves modeling different camera transformations and depth ambiguities. In contrast, for recognition, dataset unification involves merging different *semantic* concepts. Lambert et al. (2020) manually unified the taxonomies of 7 semantic segmentation datasets and used Amazon Mechanical Turk to resolve inconsistent annotations between datasets. In contrast, we propose to learn a label space from visual data automatically, without requiring any manual effort.

Wang et al. (2019) train a universal object detector on multiple datasets, and gain robustness by joining diverse sources of supervision. This is similar to our split classifier baseline, while they work on small datasets and didn’t model the training differences between different datasets. Both Wang et al. (2019) and Lambert et al. (2020) observe a performance drop in a single unified model. With our dedicated training framework, this is not the case: our unified model performs as well as single-dataset models on the training datasets. Also, these multi-headed models produce a dataset-specific prediction for each input image. When evaluated in-domain, they require knowledge of the test domain. When evaluated out-of-domain, they produce multiple outputs for a single concept. This limits their generality and usability. Our approach, on the other hand, unifies visual concepts in a single label space and yields a single consistent model that does not require knowledge of the test domain and can be deployed cleanly in new domains.

Zhao et al. (2020) trains a universal detector on multiple datasets: COCO (Lin et al., 2014), Pascal VOC (Everingham et al., 2010), and SUN-RGBD (Song et al., 2015), with under 100 classes in total. They manually merge the taxonomies and then train with cross-dataset pseudo-labels generated by dataset-specific models. The pseudo-label idea is complementary to our work. Our unified label space learn-

ing removes the manual labor, and works on a much larger scale: we unify COCO, Objects365, and OpenImages, with more complex label spaces and 900+ classes.

YOLO9000 (Redmon & Farhadi, 2017) combines detection and classification datasets to expand the detection vocabulary. LVIS (Gupta et al., 2019) extends COCO annotations to > 1000 classes in a federated way. Our approach of fusing multiple annotated datasets is complementary and can be operationalized with no manual effort to unify disparate object detection datasets.

**Zero-shot classification and detection** reasons about novel object categories outside the training set (Fu et al., 2018; Bansal et al., 2018). This is often realized by representing a novel class by a semantic embedding (Norouzi et al., 2014) or auxiliary attribute annotations (Farhadi et al., 2009). In zero-shot detection, Bansal et al. (2018) proposed a statically assigned background model to avoid novel classes being detected as background. Rahman et al. (2019) used test-time training to progressively generate new class labels based on word embeddings. Li et al. (2019) leveraged external text descriptions for novel objects. Our program is complementary: we aim to build a sufficiently large label space by merging diverse detection datasets during training, such that the trained detector transfers well across domains even without machinery such as word embeddings or attributes. Such machinery can be added, if desired, to further expand the model’s vocabulary.

## 3. Preliminaries

Object detection aims to predict a location  $b_i \in \mathbb{R}^4$  and a classwise detection score  $d_i \in \mathbb{R}^{|L|}$  for each object  $i$  in image  $I$ . The detection score describes the confidence that a bounding box belongs to an object with label  $c \in L$ , where  $L$  is the set of all classes (label space) of the dataset  $\mathcal{D}$ .

Many existing works on object detection focus on the COCO dataset (Lin et al., 2014), which contains balanced annotations for 80 common object classes. This class balance simplifies training and yields good generalization. Training an object detector on COCO follows a simple recipe: Minimize a loss  $\ell$ , usually box-level log-likelihood, over an sampled image  $\hat{I}$  and its corresponding annotated bounding boxes annotations  $\hat{B}$  from the dataset  $\mathcal{D}$ :

$$\min_{\Theta} \mathbb{E}_{(\hat{I}, \hat{B}) \sim \mathcal{D}} \left[ \ell(\mathcal{M}(\hat{I}; \Theta), \hat{B}) \right]. \quad (1)$$

Here,  $\hat{B}$  contains class-specific box annotations. The loss  $\ell$  operates on sets of outputs and annotations, and matches them using an overlap criterion.

Let’s now consider training a detector on multiple datasets  $\mathcal{D}_1, \mathcal{D}_2, \dots$ , each with their own label space  $L_1, L_2, \dots$ . A natural way to train on multiple datasets is to simply

combine all annotations of all datasets into a much larger dataset  $\mathcal{D} = \mathcal{D}_1 \cup \mathcal{D}_2 \cup \dots$ , and merge their label spaces  $L = L_1 \cup L_2 \cup \dots$ . Labels that repeat across datasets are merged. We then optimize the same loss with more data:

$$\min_{\Theta} \mathbb{E}_{(\hat{I}, \hat{B}) \sim \mathcal{D}_1 \cup \mathcal{D}_2 \cup \dots} \left[ \ell(\mathcal{M}(\hat{I}; \Theta), \hat{B}) \right]. \quad (2)$$

This has shown promise on smaller, evenly distributed datasets (Wang et al., 2019; Wu et al., 2019; Everingham et al., 2010). It has the advantage that shared classes between the datasets train on a larger set of annotations. However, modern large-scale detection datasets feature more natural class distributions that are imbalanced. Objects365 (Shao et al., 2019) contains  $5 \times$  more images than COCO and OpenImages (Kuznetsova et al., 2020) is  $18 \times$  larger than COCO. While the top 20% of classes in Objects365 and OpenImages contain  $19 \times$  and  $20 \times$  more images than COCO, respectively, the bottom 20% are actually smaller than COCO classes. This imbalance in class distributions and dataset sizes all but guarantees that a simple concatenation of datasets will not work. In fact, not even the same loss (1) works for all datasets. Most successful Objects365 models (Gao et al., 2019) employ class-aware sampling (Shen et al., 2016). OpenImages models treat rare classes differently (Tan et al., 2020) and model the hierarchy of classes in the loss (Peng et al., 2020).

This suggests that training a detector  $M_k$  on a dataset  $D_k$  requires a dataset-specific loss  $\ell_k$ :

$$\min_{\Theta} \mathbb{E}_{(\hat{I}, \hat{B}) \sim \mathcal{D}_k} \left[ \ell_k(\mathcal{M}_k(\hat{I}; \Theta), \hat{B}) \right]. \quad (3)$$

No single loss generalizes to all datasets. In the next section, we present a different view of multi-dataset training and show how to train a model that performs well on all datasets.

## 4. Training a multi-dataset detector

Our goal is to train a single detector  $\mathcal{M}$  on  $K$  datasets  $\mathcal{D}_1, \dots, \mathcal{D}_K$  with label spaces  $L_1, \dots, L_K$ , and dataset-specific training objectives  $\ell_1, \dots, \ell_K$ . Our core insight is that we can train a unified detector in the same way as we train multiple dataset-specific detectors separately, as long as we do not attempt to merge label spaces between different datasets. This can be considered training  $K$  dataset-specific detectors  $\mathcal{M}_1, \dots, \mathcal{M}_K$  in parallel, while *sharing their backbone architecture*  $\mathcal{M}$ . Each dataset-specific architecture shares all but the last layer with the common backbone. Each dataset uses its own classification layer at the end. We call this a **partitioned detector** (Figure 2b). We train a partitioned detector over all datasets by minimizing the  $K$  dataset-specific losses:

$$\min_{\Theta} \mathbb{E}_{\mathcal{D}_k} \left[ \mathbb{E}_{(\hat{I}, \hat{B}) \sim \mathcal{D}_k} \left[ \ell_k(\mathcal{M}_k(\hat{I}; \Theta), \hat{B}) \right] \right]. \quad (4)$$

Here, evenly sampling datasets, i.e. showing the partitioned detector the same number of images from each dataset, works best empirically, as we will show in Section 5.

While the partitioned detector learns to detect all classes, it still produces different dataset-specific outputs. For example, it predicts a COCO-person separately from an Objects365-Person, etc. Next we show how to convert this partitioned model into a joint detector that reasons about a *unified* set of output labels  $L = L_1 \cup L_2 \cup \dots$ .

### 4.1. Learning a unified label space

Consider multiple datasets, each with its own label space  $L_1, L_2, \dots$ . Our goal is to jointly learn a common label space  $L$  for all datasets, and define a mapping between this common label space and dataset-specific labels  $\mathcal{T}_k : L \rightarrow L_k$ . Mathematically,  $\mathcal{T}_k \in \{0, 1\}^{|L_k| \times |L|}$  is a Boolean linear transformation. In this work, we only consider direct mappings. Each joint label  $c \in L$  maps to at most one dataset-specific label  $\hat{c} \in L_k$ :  $\mathcal{T}_k^\top \mathbf{1} \leq \mathbf{1}$ . I.e., no dataset contains duplicated classes itself. Also, each dataset-specific label matches to exactly one joint label:  $\mathcal{T}_k \mathbf{1} = \mathbf{1}$ . In particular, we do not hierarchically relate concepts across datasets. When there are different label granularities, we keep them all in our label-space, and expect to predict all of them<sup>1</sup>.

Given a set of partitioned detector outputs  $d_i^1 \in \mathbb{R}^{|L_1|}, d_i^2 \in \mathbb{R}^{|L_2|}, \dots$  for a bounding box  $b_i$ , we build a joint detection score  $d_i$  by simply averaging the outputs of common classes:

$$d_i = \frac{\sum_k \mathcal{T}_k^\top d_i^k}{\sum_k \mathcal{T}_k^\top \mathbf{1}}, \quad (5)$$

where the division is elementwise. Figure 2c provides an overview. From this joint detector, we recover dataset-specific outputs  $\hat{d}_i^k = \mathcal{T}_k d_i$ . Our goal is to find a set of mappings  $\mathcal{T} = [\mathcal{T}_1^\top, \dots, \mathcal{T}_N^\top]$  and implicitly define a joint label-space  $L$  such that the joint classifier does not degrade in performance.

Simple baselines include hand-designed mappings  $\mathcal{T}$  and label spaces  $L$  (Lambert et al., 2020; Zhao et al., 2020), or language-based merging. One issue with these techniques is that word labels are ambiguous. Instead, we let the data speak and optimize a label space automatically based on correlations in the firings of a pre-trained partitioned detector on different images, which is a proxy for perceptual similarity.

For a specific output class  $c$ , let  $\mathcal{L}_c$  be a loss function that measures the quality of the merged label space  $d_i$  and its re-projections  $\hat{d}_i^k$  compared to the original disjoint label-

<sup>1</sup>This follows the official evaluation protocol of OpenImages (Kuznetsova et al., 2020).

## Simple multi-dataset detection

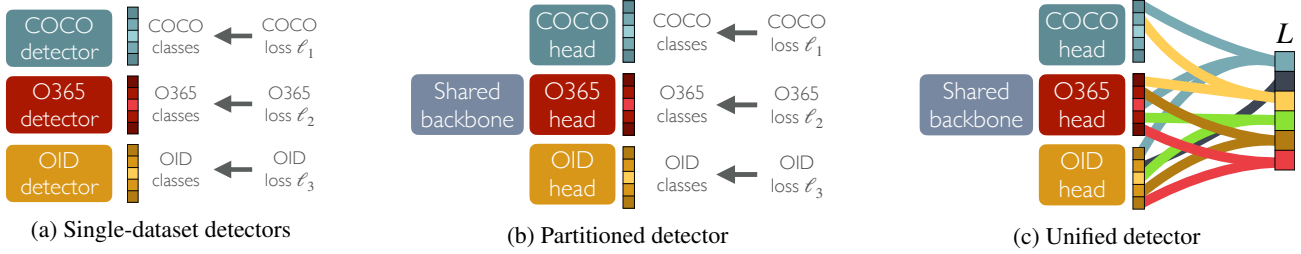


Figure 2. Standard detectors (a) are trained on one dataset with a dataset-specific loss. We train a single partitioned detector (b) on multiple datasets with shared backbone, dataset-specific outputs and loss. Finally, we unify the outputs of the partitioned detector in a common taxonomy completely automatically (c).

space  $d_i^k$  on a single box  $i$ . Let  $D^k = [d_1^k, d_2^k, \dots]$  be the outputs of the partitioned detection head for dataset  $\mathcal{D}_k$ . Let  $D = \frac{\sum_k \mathcal{T}_k^\top D^k}{\sum_k \mathcal{T}_k^\top \mathbf{1}}$  be the merged detection scores, and  $\tilde{D}^k = \mathcal{T}_k D$  be the reprojection. Our goal is to optimize this loss over all detector outputs given the Boolean constraints on our mapping

$$\begin{aligned} \text{minimize}_{L, \mathcal{T}} \quad & E_{\mathcal{D}_k} \left[ \sum_{c \in L_k} \mathcal{L}_c(D_c^k, \tilde{D}_c^k) \right] + \lambda |L| \quad (6) \\ \text{subject to} \quad & \mathcal{T}_k \mathbf{1} = \mathbf{1} \quad \text{and} \quad \mathcal{T}_k^\top \mathbf{1} \leq \mathbf{1} \quad \forall k. \end{aligned}$$

The cardinality penalty  $\lambda |L|$  encourages a small and compact label space. A factorization of the loss  $\mathcal{L}_c$  over the output space  $c \in L_k$  may seem restrictive. However, it does include the most common loss functions in detection: score distortion and Average Precision (AP). Section 4.2 discusses the exact loss functions used in our optimization.

Objective 6 mixes combinatorial optimization over  $L$  with a 0-1 integer program over  $\mathcal{T}$ . However, there is a simple reparametrization that lends itself to efficient optimization.

First, observe that the label set  $L$  simply corresponds to the number of columns in  $\mathcal{T}$ . Furthermore, we merge at most one label per dataset  $\mathcal{T}_k^\top \mathbf{1} \leq \mathbf{1}$ . Hence, for each dataset  $\mathcal{D}_k$  a column  $\mathcal{T}_k(c) \in \mathbb{T}_k$  takes one of  $|\hat{L}_k| + 1$  values:  $\mathbb{T}_k = \{\mathbf{0}, \mathbf{1}_1, \mathbf{1}_2, \dots\}$ , where  $\mathbf{1}_i \in \{0, 1\}^{|\hat{L}_k|}$  is an indicator vector of the  $i$ -th element. Each column  $\mathcal{T}(c) \in \mathbb{T}$  then only chooses from a small set of potential values  $\mathbb{T} = \mathbb{T}_1 \times \mathbb{T}_2 \times \dots$ , where  $\times$  represents the Cartesian product. Instead of optimizing over the label set  $L$  and transformation  $\mathcal{T}$  directly, we instead use combinatorial optimization over the potential column values of  $\mathbf{t} \in \mathbb{T}$ . Let  $x_{\mathbf{t}} \in \{0, 1\}$  be the indicator of combination  $\mathbf{t} \in \mathbb{T}$ .  $x_{\mathbf{t}} = 1$  means we apply the class combination specified by  $\mathbf{t}$ , and otherwise not. In this formulation, the constraint  $\mathcal{T}_k \mathbf{1} = \mathbf{1} \forall_k$  translates to  $\sum_{\mathbf{t} \in \mathbb{T} | \mathbf{t}(c)=1} x_{\mathbf{t}} = 1$  for all dataset-specific labels  $c$ . Furthermore, the objective of the optimization

simplifies to

$$\sum_{\mathbf{t} \in \mathbb{T}} x_{\mathbf{t}} E_{\mathcal{D}_k} \left[ \underbrace{\sum_{c \in L_k | \mathbf{t}(c)=1} \mathcal{L}_c(D_c^k, \tilde{D}_c^k)}_{c_{\mathbf{t}}} \right] + \lambda \sum_{\mathbf{t} \in \mathbb{T}} x_{\mathbf{t}}. \quad (7)$$

Crucially, the merge cost  $c_{\mathbf{t}}$  can be precomputed for any subset of labels  $\mathbf{t}$ . This leads to a compact integer linear programming formulation of objective 6:

$$\begin{aligned} \text{minimize}_x \quad & \sum_{\mathbf{t} \in \mathbb{T}} x_{\mathbf{t}} (c_{\mathbf{t}} + \lambda) \\ \text{subject to} \quad & \sum_{\mathbf{t} \in \mathbb{T} | \mathbf{t}(c)=1} x_{\mathbf{t}} = 1 \quad \forall c \quad (8) \end{aligned}$$

For two datasets, the above objective is equivalent to a weighted bipartite matching. For a higher number of datasets, it reduces to weighted graph matching and is NP-hard, but is practically solvable with integer linear programming (Linderoth & Ralphs, 2005).

One drawback of the combinatorial reformulation is that the set of potential combinations  $\mathbb{T}$  grows exponentially in the datasets used:  $|\mathbb{T}| = O(|\hat{L}_1| |\hat{L}_2| |\hat{L}_3| \dots)$ . However, most merges  $\mathbf{t} \in \mathbb{T}$  are bad and incur a large merge cost  $c_{\mathbf{t}}$ . The supplementary material presents a linear-time greedy enumeration algorithm for low-cost merges. Considering only low-cost matches, standard integer linear programming solvers find an optimal solution within seconds for all label spaces we tried, even for  $|L| > 600$  and up to 6 datasets.

### 4.2. Loss functions

The loss function in our constrained objective 6 is quite general and captures a wide range of commonly used losses. We highlight two: an unsupervised objective based on the distortion between partitioned and unified outputs, and Average Precision (AP) on a validation set.

**Distortion** measures the difference in detection scores between partitioned and unified detectors:

$$\mathcal{L}_c^{\text{dist}}(D_c^k, \tilde{D}_c^k) = \left( D_c^k - \tilde{D}_c^k \right)^2. \quad (9)$$

A drawback of this distortion measure is that it does not take task performance into consideration when optimizing the joint label space.

**Average Precision.** Given a reprojected dataset-specific output  $\tilde{D}_c^k$ , we can measure the average precision  $\text{AP}_c(\tilde{D}_c^k)$  of each output class  $c$  on the validation set of  $\mathcal{D}_k$ . Our loss measures the improvement in AP:

$$\mathcal{L}_c^{\text{AP}}(D_c^k, \tilde{D}_c^k) = \frac{1}{|L_k|} \left( \text{AP}_c(D_c^k) - \text{AP}_c(\tilde{D}_c^k) \right). \quad (10)$$

The AP computation is computationally quite expensive. We will provide an optimized joint evaluation in our code.

These two loss functions allow us to train a partitioned detector and merge its output space after training, either maximizing the original evaluation metric (AP) or minimizing the change incurred by the unification.

## 5. Experiments

Our goal is to facilitate the training of a single model that performs well across datasets. In this section, we first introduce our dataset setup and implementation details. In Section 5.1, we analyze our key design choices for a partitioned detector baseline. In Section 5.2, we evaluate our unified detector and our unified label space learning algorithm. We further evaluate the unified detector in new test datasets in a zero-shot setting (Section 5.3) and report its performance in the ECCV 2020 Robust Vision Challenge (Section 5.4).

**Datasets.** Our main training datasets are adopted from the ECCV 2020 Robust Vision Challenge (RVC). These are four large object detection datasets: COCO (Lin et al., 2014), OpenImages (Kuznetsova et al., 2020), Objects365 (Shao et al., 2019), and optionally Mapillary (Neuhold et al., 2017). To evaluate the generalization ability of the models, we follow MSeg (Lambert et al., 2020) to set up a zero-shot cross-dataset evaluation protocol: we evaluate models on new test dataset *without training on them*. Specifically, we test on VIPER (Richter et al., 2017), Cityscapes (Cordts et al., 2016), ScanNet (Dai et al., 2017), WildDash (Zendel et al., 2018), KITTI (Geiger et al., 2012), Pascal VOC (Everingham et al., 2010), and CrowdHuman (Shao et al., 2018). A detailed description of all datasets is contained in the supplement. In our main evaluation, we use large and general datasets: COCO, Objects365, and OpenImages. Mapillary is relatively small and is specific to traffic scenes; we only add it for the RVC and cross-dataset experiments.

For each dataset, we use its official evaluation metric: for COCO, Objects365, and Mapillary, we use mAP at IoU thresholds 0.5 to 0.95. For OpenImages, we use the official modified mAP@0.5 that excludes unlabeled classes and enforces hierarchical labels (Kuznetsova et al., 2020). For the

	COCO	O365	OImg	mean
Simple merge (Wang et al., 2019)	34.2	14.6	50.8	33.2
w/ uniform dataset sampling	41.1	16.5	46.0	34.5
w/ class-aware sampling	35.3	18.5	61.8	38.5
w/ dataset+class-aware sampling	<b>41.8</b>	20.3	60.0	40.6
Partitioned detector (ours)	<b>41.8</b>	<b>20.6</b>	<b>62.7</b>	<b>41.7</b>

Table 1. Ablation of our multi-dataset training strategies. We start with simple merging of datasets (Wang et al., 2019), then add a uniform sampling of images between different training datasets (second row), class-aware sampling within Objects365 and OpenImages (third row), and both sampling strategies (forth row). Our partitioned detector combines these sampling strategies with a dataset-specific loss (last row).

small datasets in cross-dataset evaluation, we use mAP at IoU threshold 0.5 for consistency with PascalVOC (Everingham et al., 2010).

**Implementation details.** We use the CascadeRCNN detector (Cai & Vasconcelos, 2019) with a shared region proposal network (RPN) across datasets. We evaluate two models in our experiments: a partitioned detector (i.e., detector with dataset-specific output heads) and a unified model). For the partitioned detector, the last classification layer of each cascade stage is split between datasets. The unified model uses the CascadeRCNN as is.

Our implementation is based on Detectron2 (Wu et al., 2019). We adopt most of the default hyperparameters for training. We use the standard data augmentation, including random flip and scaling of the short edge in the range [640, 800]. We use SGD with base learning rate 0.01 and batch size 16 over 8 GPUs. We use ResNet50 (He et al., 2016) as the backbone in our controlled experiments unless specified otherwise. We use a 2× training schedule (180k iterations with learning rate dropped at the 120k and 160k iterations) (Wu et al., 2019) in most experiments unless specified otherwise, regardless of the training data size.

### 5.1. Multi-dataset detection

We first evaluate the partitioned detector. We use dataset-specific outputs and do not merge classes between different datasets. During evaluation, we assume the target dataset is known and only look at the corresponding output head. As discussed in Section 4, our baseline highlights two basic components: uniform sampling of images between datasets and dataset-specific training objective. For these experiments we distinguish between modifications of the objective that merely sample data differently within each dataset (e.g. class-aware sampling), and changes to the loss functions (e.g. hierarchical losses).

We start from the baseline of Wang et al. (2019); Wu et al. (2019). They simply collect all data from all datasets and

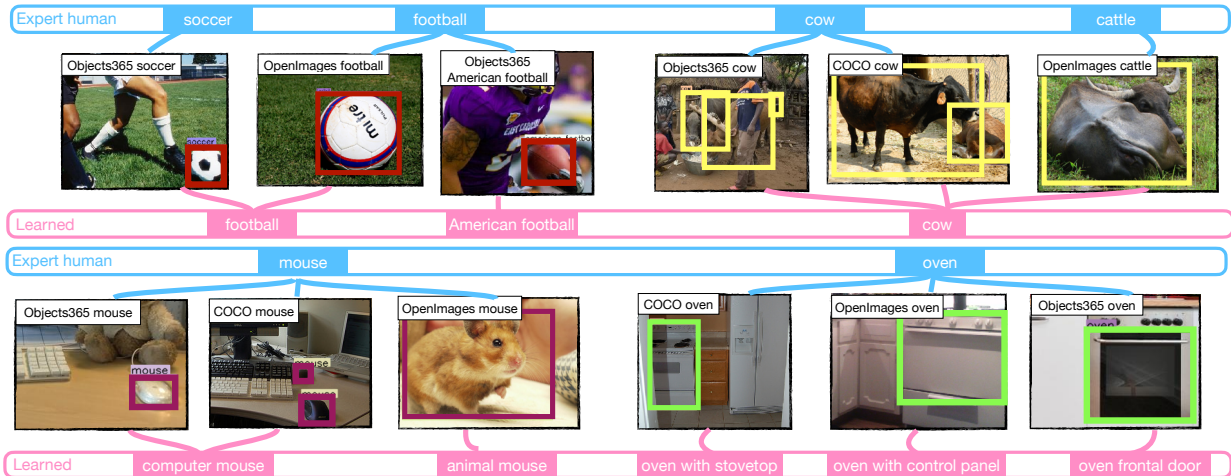


Figure 3. Some differences between an expert-designed label space provided as part of the ECCV 2020 Robust Vision Challenge (top of each row, blue) and our learned label space (bottom of each row, pink). Zoom in for details.

train with a common loss. As is shown in Table 1, this biases the model to large datasets (OpenImages) and yields low performance for relatively small datasets (COCO). Sampling datasets uniformly (second row) trades the performance on smaller datasets with large datasets, and overall improves performance. On the other hand, both OpenImages and Objects365 are long-tailed and best train with advanced inter-dataset sampling strategy (Shen et al., 2016; Peng et al., 2020), namely class-aware sampling. Class-aware sampling significantly improves accuracy on OpenImages and Objects365. Combining the uniform dataset sampling and the intra-dataset class-aware sampling gives a further boost. Finally, OpenImages (Kuznetsova et al., 2020) requires predicting a label hierarchy. For example, it requires predicting “vehicle” and “car” for all cars. This breaks the default cross-entropy loss that assumes exclusive class labels per object. We instead use a dedicated hierarchy-aware sigmoid cross-entropy loss for OpenImages (Kuznetsova et al., 2020). Specifically, for an annotated class label in OpenImages, we set all its parent classes as positives and ignore the losses over its descendant classes. Our partitioned detector combines both sampling strategies and the dataset-specific loss. The hierarchy-aware loss yields a significant +2.7mAP improvement on OpenImages alone, and does not degrade other datasets.

**Dateset-specific vs. partitioned detection.** In our partitioned detector, training on multiple datasets resembles

training separate individual models but with a shared detector. Table 2 compares training a partitioned detector on all datasets with dataset-specific models. We compare detectors under different training schedules ( $n \times$  the COCO default schedule). Each of the three dataset-specific models sees the same number of gradient updates as our partitioned detector. In a  $2 \times$  training schedule (180k iterations), single-dataset models generally perform better than a partitioned model, as each dataset is only trained for a  $\frac{1}{3} \times$  schedule in the partitioned model. At a  $6 \times$  schedule, the partitioned detector starts to match dataset-specific models, and outperforms  $2 \times$  dataset-specific models under the same total iterations. In a  $8 \times$  schedule, all models converge. Here the partitioned detector surpasses the single-dataset model on COCO and OpenImages, and closely matches the Objects365 model.

## 5.2. Unified multi-dataset detection

Next, we evaluate different unification strategies for the label space.

**Unification strategies.** We run our label space learning algorithm from Section 4.1 based on the output of a partitioned detector with a ResNeSt backbone (Zhang et al., 2020) trained on COCO, Objects365, and OpenImages, with a total of 945 disjoint classes. The hyperparameters are  $\lambda = 0.5$  and  $\tau = 0.2$ . The optimization ends up with a unified label space with cardinality  $|L| = 701$ . we compare our

	2×			6×			8×		
	COCO	Objects365	OImg.	COCO	Objects365	OImg.	COCO	Objects365	OImg.
Partitioned detector	<b>41.8</b>	20.6	62.7	<b>44.6</b>	23.6	64.8	<b>45.5</b>	24.6	<b>66.0</b>
COCO	41.5	-	-	42.5	-	-	42.5	-	-
Objects365	-	<b>23.8</b>	-	-	<b>25.0</b>	-	-	<b>24.9</b>	-
OpenImages	-	-	<b>64.6</b>	-	-	<b>65.4</b>	-	-	65.7

Table 2. Comparison of a partitioned detector to single-dataset models under different training schedules in terms of validation mAP.

	COCO	O365	OImg.	mean
GloVe embedding	41.6 $\pm$ 0.00	20.3 $\pm$ 0.12	62.4 $\pm$ 0.06	41.4 $\pm$ 0.05
Learned, distortion	41.6 $\pm$ 0.15	20.7 $\pm$ 0.06	62.6 $\pm$ 0.06	41.7 $\pm$ 0.09
Learned, AP (ours)	<b>41.9<math>\pm</math>0.10</b>	<b>20.8<math>\pm</math>0.10</b>	<b>63.0<math>\pm</math>0.21</b>	<b>41.9<math>\pm</math>0.02</b>
Expert human	41.5 $\pm$ 0.06	20.7 $\pm$ 0.06	62.6 $\pm$ 0.06	41.6 $\pm$ 0.04

Table 3. Evaluation of unified label spaces. We measure mAP on the validation sets of the training domains. We compare to a language-based baseline (GloVe) and a manual unification by a human expert. Each model is a ResNet-50 CascadeRCNN trained in a  $2\times$  schedule. We show the mean and standard deviation based on 3 repeated runs under different random seeds.

automated data-driven unification to human and language-based baselines. We use the official manually-crafted ECCV RVC taxonomy as the human expert baseline<sup>2</sup>.

Over two-thirds of our learned label space agrees with the human expert. Figure 3 highlights some of the differences. Our unification successfully groups similar concepts with different descriptions (“Cow” and “Cattle”), and is not distracted by spurious linguistic matches (“American football” and “football”). Interestingly, the learned label space splits the “oven” classes from COCO, Objects365, and OpenImages, even though they share the same word. A visual examination reveals that they are visually dissimilar due to different underlying definitions of the “oven” concept in the different datasets: COCO ovens include the cooktop, OpenImages ovens include the control panel, and Objects365 ovens are just the front door. Our data-driven taxonomy reconciliation is able to detect such distinctions, which are missed by word-level approaches.

We next quantitatively compare our learned label space with alternatives. For each label space, we retrain a multi-dataset detector with that label space. During training, as with our partitioned model, we only apply training losses to the classes that are annotated in the source dataset. We compare our learned label space to a “best effort” human baseline and a language-based baseline. For the language-based baseline, we replace the cost measurement defined in Section 4.2 with the cosine distance between the GloVe word embeddings (Pennington et al., 2014), and run the same integer linear program. Table 3 shows the results. We repeat the training for three runs with different random seeds and report the mean and standard deviation. The four label spaces agree on most classes and the overall mAP is thus close. Our automatically constructed label space consistently outperforms the human expert baseline, with a healthy 0.3 mAP margin on average. The improvement appears statistically stable under multiple training runs. Notably, the relative improvement of our model over the expert is larger than the expert’s improvement over the language-based baseline.

<sup>2</sup>[https://github.com/ozendelait/rvc\\_devkit/blob/master/objdet/obj\\_det\\_mapping.csv](https://github.com/ozendelait/rvc_devkit/blob/master/objdet/obj_det_mapping.csv)

	COCO	O365	OImg.	mean
Unified (partitioned)	44.4	23.6	65.3	44.4
Unified (retrained)	45.4	24.4	66.0	45.3
Partitioned (oracle)	45.5	24.6	66.0	45.4
Ensemble (oracle)	42.5	24.9	65.7	44.4

Table 4. Validation mAP on training domains for our unified detector (top), the same detector retrained on the joint taxonomy (second), a partitioned detector knowing the target domain (third), and an ensemble of three dataset-specific detectors (bottom). The bottom two rows require a known test dataset source and the top two rows do not. All models use a ResNet-50 CascadeRCNN trained in an  $8\times$  schedule.

**Unified vs. partitioned detectors.** We next compare a partitioned detector, a unified detector with and without retraining using the joint taxonomy, and an ensemble of dataset-specific detectors. Note that the partitioned detector and the ensemble need to know the target domain at test time, while the unified models do not. This means that the unified models can be deployed zero-shot in new domains, while the alternatives must know which domain they are in. Table 4 shows the results. A partitioned detector outperforms a dataset-specific ensemble under the same experimental conditions (known test domain), especially on the “small” COCO dataset. An offline unification loses some accuracy, but this is regained when retraining the model under the unified taxonomy. Crucially, the unified models do not need to know what domain they are in at test time.

### 5.3. Zero-shot cross-dataset evaluation

We evaluate the generalization ability of object detectors by evaluating them in new test domains not seen during training. In this setting, we do not assume to know the test classes ahead of time. To allow for a fair and unbiased evaluation, we use a simple language-based matching to find the test-to-train label correspondence. Specifically, we calculate the GloVe (Pennington et al., 2014) word embedding distances between each test label and the training label, and match the test label to its closest training label. If multiple training labels match, we break ties in a fixed order: COCO, Objects365, OpenImages, and Mapillary<sup>3</sup>.

We compare both our multi-dataset models (partitioned or unified) to single-dataset models. We use all four RVC training sets to train the multi-dataset models. Specifically, we start from a  $6\times$  schedule model trained on the three large datasets, and add Mapillary (Neuhold et al., 2017) in a  $2\times$  fine-tuning schedule with  $10\times$  smaller learning rate. We compare all models under the same schedule<sup>4</sup>,

<sup>3</sup>We also tried evaluating under different orders, and find the listed order to perform best for all methods.

<sup>4</sup>except for the Mapillary model, for which a  $2\times$  schedule performs better than longer schedules.

### Simple multi-dataset detection

	VOC	VIPER	Cityscapes	ScanNet	WildDash	CrowdH.	KITTI	mean
COCO	80.0	13.9	39.6	17.4	25.9	<b>73.9</b>	30.5	40.2
Objects365	71.9	20.7	43.4	24.9	27.6	71.8	32.2	41.8
OpenImages	64.4	10.4	29.8	24.2	20.3	66.7	21.8	33.9
Mapillary	11.4	15.2	44.7	0.0	23.4	49.3	37.8	26.0
Ensemble	79.7	16.8	46.0	30.1	32.1	<b>73.9</b>	34.3	44.7
Partitioned	<b>83.1</b>	20.9	48.4	<b>32.2</b>	34.4	70.0	38.9	46.8
Unified (retrained)	<b>82.9</b>	<b>21.3</b>	<b>52.6</b>	29.8	<b>34.7</b>	70.7	<b>39.9</b>	<b>47.3</b>
Dataset-specific	80.3	31.8	54.6	44.7	-	80.0	-	-

Table 5. Zero-shot cross-dataset object detection performance on the validation sets of datasets that were not seen during training. We compare models trained on each single training dataset (top 4 rows), the ensemble of the 4 single dataset models (5th row), a partitioned detector (6th row), and the unified detector with our learned unified label space (7th row). For reference, we show the “oracle” models that are trained on the training set of each test dataset on the bottom row. The columns refer to test datasets. Each model is a ResNet-50 CascadeRCNN trained until converge or at most an  $8\times$  schedule.

hyperparameters, and detection models. In addition, we also compare to the ensemble of the four single-dataset models trained analogously to the partitioned model. For reference, we also show the performance of detectors trained on the training set of each test dataset. This serves as an oracle “upper bound” that has seen the test domain and label space. Note that KITTI and WildDash are small and do not have a validation set. We thus directly evaluate on the training set and do not provide the oracle model.

Table 5 shows the results. The COCO model exhibits reasonable performances of some test datasets, such as Pascal VOC and CrowdHuman. However, its performance is less than satisfactory on datasets such as ScanNet, whose label space differs significantly from COCO. Training on the more diverse Objects365 dataset yields higher accuracy in the indoor domain, but loses ground on VOC and CrowdHuman, which are more similar to COCO. Training on all datasets, either with a partitioned detector or a unified one yields generally good performance on all test datasets. Notably, both our detectors perform better than the ensemble of the 4 single dataset models, showing that the multi-dataset models learned more general features. On Pascal VOC, both multi-dataset models outperform the VOC-trained upper-bound without ever seeing VOC training images. Our unified model outperforms the partitioned detector overall and operates on a single unified taxonomy.

#### 5.4. ECCV Robust Vision Challenge

We submitted a model trained with the presented approach to the ECCV 2020 Robust Vision Challenge (RVC). We used a heavy ResNeSt200 backbone (Zhang et al., 2020) and followed the same training procedure as in Section 5.2 with an  $8\times$  schedule. We used a unified label space of 682 classes learned with the distortion loss. The training took  $\sim 16$  days on a server with 8 Quadro RTX 6000 GPUs. Table 6 summarizes the results of the challenge. Our model won the challenge, outperforming all other RVC entries on

	COCO	OImg.	Mapillary	O365
Ours	<b>52.9</b>	<b>60.6/56.8</b>	<b>25.3</b>	<b>33.7</b>
WiseDet_RVC	40.0	56.1/53.3	22.5	-
FRCNN_R50_GN_RVC	34.0	21.4/19.9	8.1	-
DetectoRS	<b>53.3</b>	-	-	-
TSD	-	60.5/-	-	-
CACascade RCNN	-	-	-	31.6

Table 6. RVC results: COCO test-challenge set, OpenImages challenge 2019 test sets (public test set/ private test set), Mapillary test set, and Objects365 validation set. Top: results of RVC challenge participants. Bottom: published state-of-the-art models on each specific dataset (without model ensembles or test-time augmentation). Objects365 was initially part of the challenge but was removed in the final evaluation.

all datasets by a large margin. Notably, WiseDet\_RVC used a stronger detector (Qiao et al., 2020), but is trained under a uniform sampling strategy and uses the same training loss for all datasets. We also compare to state-of-the-art results on each individual dataset. On COCO, our result compares well to DetectoRS (Qiao et al., 2020), which is by default 2.4 mAP higher than our ResNeSt200 backbone (50.9 mAP) (Zhang et al., 2020). On OpenImages, our result matches the best single model in the OpenImages 2019 Challenge, TSD (Song et al., 2020), with a comparable backbone (SENet154-DCN (Hu et al., 2018)). On Objects365, we outperform the 2019 challenge winner (Gao et al., 2019) by 2 mAP points. We also won the RVC instance segmentation challenge, see the supplement for details.

## 6. Conclusion

We presented a simple approach for training an object detector across multiple datasets and automatically constructing a unified taxonomy for deploying the detector without knowledge of the test-time domain. Our models match dataset-specific performance in training domains, and outperform all baselines when evaluated on new test domains.

## References

- Bansal, A., Sikka, K., Sharma, G., Chellappa, R., and Divakaran, A. Zero-shot object detection. In *ECCV*, 2018.
- Cai, Z. and Vasconcelos, N. Cascade r-cnn: High quality object detection and instance segmentation. *TPAMI*, 2019.
- Cordts, M., Omran, M., Ramos, S., Rehfeld, T., Enzweiler, M., Benenson, R., Franke, U., Roth, S., and Schiele, B. The cityscapes dataset for semantic urban scene understanding. In *CVPR*, 2016.
- Dai, A., Chang, A. X., Savva, M., Halber, M., Funkhouser, T., and Nießner, M. Scannet: Richly-annotated 3d reconstructions of indoor scenes. In *CVPR*, 2017.
- Everingham, M., Van Gool, L., Williams, C. K., Winn, J., and Zisserman, A. The PASCAL visual object classes (VOC) challenge. *IJCV*, 2010.
- Farhadi, A., Endres, I., Hoiem, D., and Forsyth, D. Describing objects by their attributes. In *CVPR*, 2009.
- Fu, Y., Xiang, T., Jiang, Y.-G., Xue, X., Sigal, L., and Gong, S. Recent advances in zero-shot recognition: Toward data-efficient understanding of visual content. *IEEE Signal Processing Magazine*, 2018.
- Gao, Y., Shen, H., Zhong, D., Wang, J., Liu, Z., Bai, T., Long, X., and Wen, S. A solution for densely annotated large scale object detection task. 2019.
- Geiger, A., Lenz, P., and Urtasun, R. Are we ready for autonomous driving? the kitti vision benchmark suite. In *CVPR*, 2012.
- Gupta, A., Dollar, P., and Girshick, R. Lvis: A dataset for large vocabulary instance segmentation. In *CVPR*, 2019.
- He, K., Zhang, X., Ren, S., and Sun, J. Deep residual learning for image recognition. In *CVPR*, 2016.
- He, K., Gkioxari, G., Dollár, P., and Girshick, R. Mask r-cnn. In *CVPR*, 2017.
- Hu, J., Shen, L., and Sun, G. Squeeze-and-excitation networks. In *CVPR*, 2018.
- Kuznetsova, A., Rom, H., Alldrin, N., Uijlings, J., Krasin, I., Pont-Tuset, J., Kamali, S., Popov, S., Mallocci, M., Kolesnikov, A., Duerig, T., and Ferrari, V. The open images dataset v4: Unified image classification, object detection, and visual relationship detection at scale. *IJCV*, 2020.
- Lambert, J., Liu, Z., Sener, O., Hays, J., and Koltun, V. MSeg: A composite dataset for multi-domain semantic segmentation. In *CVPR*, 2020.
- Li, Z., Yao, L., Zhang, X., Wang, X., Kanhere, S., and Zhang, H. Zero-shot object detection with textual descriptions. In *AAAI*, 2019.
- Lin, T.-Y., Maire, M., Belongie, S., Hays, J., Perona, P., Ramanan, D., Dollár, P., and Zitnick, C. L. Microsoft coco: Common objects in context. In *ECCV*, 2014.
- Linderoth, J. T. and Ralphs, T. K. Noncommercial software for mixed-integer linear programming. *Integer programming: theory and practice*, 3(253-303):144–189, 2005.
- Neuhof, G., Ollmann, T., Rota Bulò, S., and Kotschieder, P. The mapillary vistas dataset for semantic understanding of street scenes. In *ICCV*, 2017.
- Norouzi, M., Mikolov, T., Bengio, S., Singer, Y., Shlens, J., Frome, A., Corrado, G. S., and Dean, J. Zero-shot learning by convex combination of semantic embeddings. In *ICLR*, 2014.
- Peng, J., Bu, X., Sun, M., Zhang, Z., Tan, T., and Yan, J. Large-scale object detection in the wild from imbalanced multi-labels. In *CVPR*, 2020.
- Pennington, J., Socher, R., and Manning, C. D. Glove: Global vectors for word representation. In *EMNLP*, 2014.
- Qiao, S., Chen, L.-C., and Yuille, A. Detectors: Detecting objects with recursive feature pyramid and switchable atrous convolution. *arXiv:2006.02334*, 2020.
- Rahman, S., Khan, S., and Barnes, N. Transductive learning for zero-shot object detection. In *ICCV*, 2019.
- Ranftl, R., Lasinger, K., Hafner, D., Schindler, K., and Koltun, V. Towards robust monocular depth estimation: Mixing datasets for zero-shot cross-dataset transfer. *TPAMI*, 2020.
- Redmon, J. and Farhadi, A. Yolo9000: better, faster, stronger. In *CVPR*, 2017.
- Ren, S., He, K., Girshick, R., and Sun, J. Faster r-cnn: Towards real-time object detection with region proposal networks. In *NIPS*, 2015.
- Richter, S. R., Hayder, Z., and Koltun, V. Playing for benchmarks. In *ICCV*, 2017.
- Shao, S., Zhao, Z., Li, B., Xiao, T., Yu, G., Zhang, X., and Sun, J. Crowdhuman: A benchmark for detecting human in a crowd. *arXiv:1805.00123*, 2018.
- Shao, S., Li, Z., Zhang, T., Peng, C., Yu, G., Zhang, X., Li, J., and Sun, J. Objects365: A large-scale, high-quality dataset for object detection. In *ICCV*, 2019.

- Shen, L., Lin, Z., and Huang, Q. Relay backpropagation for effective learning of deep convolutional neural networks. In *ECCV*, 2016.
- Song, G., Liu, Y., and Wang, X. Revisiting the sibling head in object detector. In *CVPR*, 2020.
- Song, S., Lichtenberg, S. P., and Xiao, J. Sun rgb-d: A rgb-d scene understanding benchmark suite. In *CVPR*, 2015.
- Tan, J., Wang, C., Li, B., Li, Q., Ouyang, W., Yin, C., and Yan, J. Equalization loss for long-tailed object recognition. In *CVPR*, 2020.
- Wang, X., Cai, Z., Gao, D., and Vasconcelos, N. Towards universal object detection by domain attention. In *CVPR*, 2019.
- Wu, Y., Kirillov, A., Massa, F., Lo, W.-Y., and Girshick, R. Detectron2. <https://github.com/facebookresearch/detectron2>, 2019.
- Yang, G., Manela, J., Happold, M., and Ramanan, D. Hierarchical deep stereo matching on high-resolution images. In *CVPR*, 2019.
- Zendel, O., Honauer, K., Murschitz, M., Steininger, D., and Fernandez Dominguez, G. Wilddash-creating hazard-aware benchmarks. In *ECCV*, 2018.
- Zhang, H., Wu, C., Zhang, Z., Zhu, Y., Zhang, Z., Lin, H., Sun, Y., He, T., Mueller, J., Manmatha, R., et al. Resnest: Split-attention networks. *arXiv: 2004.08955*, 2020.
- Zhao, X., Schuler, S., Sharma, G., Tsai, Y.-H., Chandraker, M., and Wu, Y. Object detection with a unified label space from multiple datasets. In *ECCV*, 2020.

Dataset name	Domain	# Cat.	# Img.
<b>Train &amp; Validation</b>			
COCO	Internet images	80	118k
Objects365	Internet images	365	600k
OpenImages	Internet images	500	1.8M
Mapillary	Traffic	38	18k
<b>Test</b>			
ScanNet	Indoor	20	25k
VIPER	Virtual	10	13k
Cityscapes	Traffic	8	12k
WildDash	Traffic	13	4k
KITTI	Traffic	8	200
Pascal VOC	Internet images	20	16k
CrowdHuman	Internet images	1	15k

Table 7. Datasets we used. Top: datasets we used in training and validation, which are from the ECCV 2020 Robust Vision Challenge. Bottom: datasets we used for zero-shot cross-dataset testing.

## A. Dataset details

Table 7 lists the datasets we used in our experiments. We use the ECCV 20 Robust Vision Challenge official release of each dataset. Specifically, we use the standard 2017 train/validation split for COCO (Lin et al., 2014), the Challenge-2019 release of OpenImages (Kuznetsova et al., 2020), and the default version of Objects365 (Shao et al., 2019) and Mapillary (Neuhold et al., 2017). For ScanNet (Dai et al., 2017), as there is no standard train/validation split, we use the first 80% scenes (sorted by scene ID) as training and the last 20% scene as validation. For KITTI (Geiger et al., 2012), we used the RVC challenge version that has instance-segmentation version, which contains 200 images. For WildDash (Zendel et al., 2018), we use the public version for evaluation, and report standard mAP performance. We don’t consider the negative label metric in the official website. For CrowdHuman (Shao et al., 2018), we use the visible bounding box annotation, and report mAP instead of the missing rate as the official metric. We use the official train/validation split and the official evaluation metrics for VIPER (Richter et al., 2017), Cityscapes (Cordts et al., 2016), and Pascal VOC (Everingham et al., 2010).

## B. Computation of label space learning algorithm and pruning

The size of our optimization problem scales linearly in the number of potential merges  $|\mathbb{T}|$ , which can grow exponentially in the number of datasets. To counteract this exponential growth, we only consider sets of classes

$$\mathbb{T}' = \left\{ \mathbf{t} \in \mathbb{T} \mid \frac{c_{\mathbf{t}}}{|\mathbf{t}| - 1} \leq \tau \right\}.$$

For an aggressive enough threshold  $\tau$ , the number of potential merges  $|\mathbb{T}'|$  remains manageable. We greedily grow  $\mathbb{T}'$

by first enumerating all feasible two-class merges ( $|\mathbf{t}| = 2$ ), then three-class merges, and so on. The detailed algorithm diagram is shown in Algorithm 1. The runtime of this greedy algorithm is  $O(|\mathbb{T}'| \max_i |\hat{L}^i|)$ . In practice, the cost computation took a few seconds for the distortion loss function and about 10 minutes for the AP loss (due to the need to repeatedly recompute AP). The integer programming solver finds the optimal solution within one second in both cases.

## C. Adding new datasets to a label space

While we tend to keep the training domains and label space large and comprehensive, it is inevitable in practice that more fine-grained labels or specific testing domains are needed. Given a learned a unified label space on an existing set of training datasets, we use a simple label space expansion algorithm to allow adding more datasets and labels after the unified detector is trained.

### Algorithm 1 Learning a unified label space

**Input** :  $\{\mathbf{b}_i, \tilde{\mathbf{l}}_i\}_{i=1}^N$ : ground truth bounding boxes and labels for each of the  $N$  training datasets  
 $\{\{\tilde{\mathbf{b}}_i^{(j)}, \tilde{\mathbf{l}}_i^{(j)}\}_{j=1}^N\}_{i=1}^N$ : predicted bounding boxes with predicted classes in all datasets for each training dataset  
 $\lambda, \tau$ : hyper-parameters for algorithm

**Output** :  $L$ : unified label space

$\mathcal{T}$ : the transformation from each individual label space to the unified label space

```

1 // Compute potential merges and merge cost
 $\hat{L} = \bigcup_i \hat{L}_i$  // Short-hand used to simplify notation
 $\mathbb{T}_1 \leftarrow \{(l) \mid l \in \hat{L}\}$  // Set of single labels
Compute  $c_t$  for all single labels  $t \in \mathbb{T}$ . // 0 for most metrics
for  $n = 2 \dots N$  do
2    $\mathbb{T}_n \leftarrow \{\}$ 
   for  $t \in \mathbb{T}_{n-1}$  do
3     for  $l \in \hat{L}$  do
4       if  $l$  and all labels in  $t$  are from different datasets
5         then
6           compute  $c_{t \cup \{l\}}$ .
7           if  $\frac{c_{t \cup \{l\}}}{n-1} \leq \tau$  then
8             Add  $t \cup \{l\}$  to  $\mathbb{T}_n$ .
9           end
10        end
11     end
12  $\mathbb{T} \leftarrow \bigcup_{n=1}^N \mathbb{T}_n$ 
// Solve the ILP.
 $\mathbf{x} \leftarrow \text{ILP\_solver}(c, \mathbb{T}, \lambda)$  // Solve equation (8).
Compute  $L, \mathcal{T}$  from  $\mathbf{x}$ 
Return:  $L, \mathcal{T}$ 

```

## Simple multi-dataset detection

	COCO	CityScapes	Mapillary	VIPER	ScanNet	OpenImages	KITTI	WildDash
COCO	<b>35.6</b>	19.6	3.2	8.5	5.2	7.2	15.7	8.4
CityScapes	0.0	21.5	0.8	2.3	0.0	0.0	13.0	2.4
Mapillary	0.6	11.7	<b>10.6</b>	9.0	1.2	0.0	13.4	5.4
VIPER	0.1	2.8	1.1	<b>17.8</b>	0.0	0.0	6.5	1.4
ScanNet	0.4	0.0	0.0	0.0	<b>35.6</b>	0.0	0.0	0.0
OpenImages	12.9	9.5	1.1	3.5	1.7	<b>52.8</b>	7.2	4.9
Unified (ours)	24.0	<b>28.3</b>	8.1	16.5	28.7	41.8	<b>16.9</b>	<b>11.3</b>

Table 8. Instance segmentation performance on six training datasets and two new datasets (KITTI and WildDash). We show mask mAP on the validation set of each dataset.

	COCO	CityScapes	Mapillary	VIPER	ScanNet	OpenImages	KITTI	WildDash
Ours	33.0	29.8	13.0	18.9	20.5	35.0	23.2	21.0
seamseg_rvcsubset	-	22.1	-	-	-	-	-	20.9
EffPS_b1bs4_RVC	-	21.3	-	-	-	-	-	-

Table 9. Leaderboard of RVC instance segmentation challenge. We show results on the test set for each datasets (test-challenge for COCO and private test set for OpenImages).

Similar to our unified label space learning algorithm, we run the unified detector on the new training data. We evaluate the AP between each class in the new dataset annotation and each class in the unified label space. We merge the new class into the existing class that gives the lowest merge cost (Section. 4.2). In our experiments, add Mapillary dataset (Neuhold et al., 2017) to our label space we using the AP loss. If the cost is lower than a threshold (AP change  $< 5$  AP in our implementation). Otherwise, we append the new class to the unified label space as a single class.

### D. Discussion on label hierarchy

Different datasets may contain different label granularities for the same concept, and there exists label hierarchies inter or intra datasets. For example, Objects365 (Shao et al., 2019) does not have a “bird” category, but has more fine-grained bird species like parrot, pigeon, and swan, while most other datasets only annotate “bird”. Our label space optimization algorithm automatically handles the hierarchical label space issue: the fine-grained birds in Objects365 will not merge with COCO birds because this merge introduces many false-positives for the fine-grained birds in Objects365 and yields a large cost. Our unified label space will contain both the general “bird” class and each fine-grained class. The model trained on the unified label space is expected to predict both the coarse “bird” label and the fine-grained label in testing.

### E. Instance segmentation

We further evaluate our label space learning algorithm and unified training framework on instance segmentation. We follow the ECCV Robust vision challenge set up to use 8 datasets: COCO, OpenImages, Mapillary, ScanNet, VIPER,

CityScapes, WildDash and KITTI (the same as Table 7, except OpenImages segmentation set has 300 instead of 500 classes.). Again, we leave WildDash and KITTI as testing only as they are small and similar to CityScapes and Mapillary. We run our label space learning algorithm (Section. 4) on the remaining six datasets, resulting a unified label space of 358 classes. We use CascadeRCNN (Cai & Vasconcelos, 2019) with a standard mask head as the detector, and train a  $2\times$  schedule with ResNet50. The dataset-specific models are trained with  $1\times$  or  $2\times$  schedule depending on their size.

Table. 8 compares the unified detector (with instance segmentation) to dataset specific models. As expected, no single dataset-specific model performs well on all test domains. Our unified model performs consistently good on all training datasets. More importantly, it generalizes the best to the new test datasets (KITTI and WildDash) than any single dataset model. Table. 9 compares our method with others on the test sets of RVC instance segmentation challenge. We outperform other entries on all datasets that have a valid submission.